Leakage current, self-clearing and actuation efficiency of nanometer-thin, low-voltage dielectric elastomer transducers tailored by thermal evaporation

Tino Töpper[a], Bekim Osmani[a], Samuel Lörcher[b], and Bert Müller[a]

[a] Biomaterials Science Center, University of Basel, 4123 Allschwil, Switzerland;
[b] Chemistry Department, University of Basel, 4056 Basel, Switzerland.

ABSTRACT

The low-voltage operation is the key challenge for dielectric elastomer transducers (DET) to enter the application field of medically approved actuators or sensors, such as artificial muscles or skin. Recently, it has been successfully shown that the reduction of the elastomer film thickness to a few hundred nanometers allows for the DEA operation reaching 6 % strain using only a few volts. Molecular beam deposition (MBD) enables us to tailor elastomer films with low defect level. Combined with *in situ* spectroscopic ellipsometry, MBD is a unique method to reliably deposit polydimethylsiloxane (PDMS) thin films with true nanometer precision. The homogenous cross-linking of the PDMS film has been *in situ* realized by curing through ultraviolet (UV) radiation during deposition. We present the successful tailoring of the elastomer membrane's elastic modulus down to a few hundreds of kPa by varying the UV-irradiation density. Atomic force microscopy (AFM) nano-indentation reveals homogeneously polymerized membranes. An adhesion layer of thiol-functionalized PDMS is applied to localize gold particles of the electrode layer to prevent diffusion into the nanometer-thin elastomer film and to reduce the leakage current. The understanding of leakage currents of such nanometer-thin elastomer films is crucial to preserve the unique actuation efficiency for DETs in low-voltage operation. Leakage currents are determined for a 200 nm-thin DEA as low as 10^{-3} A/m² at applied electric fields of about 80 V/µm just before local breakdown events occur. Known as *self-clearing*, the vaporization of local defects enables to regain the functionality of the DET with subsequent reduced leakage current. AFM is utilized for the characterization of these DET low-voltage nanostructures regarding their vertical strain and actuation efficiency. A strain-to-voltage-squared (s/V^2) ratio of 755 %/kV² for a single-layer 500 nm-thin DEA is acquired - by far the highest reported (s/V^2)-value for thin-film DEAs. A two-layer DET nanostructure is compared to a single layer DET with doubled elastomer film thickness to evaluate the repeatedly discussed stiffening electrode effect. This occurs when DET nanostructures are stacked above hundreds of times, the major challenge remaining to realize biomimetic DET with forces and compliance close to the natural muscles.

Keywords: Nanometer-thin polydimethylsiloxane membranes, tailored elastic modulus, low-voltage actuators and sensors, leakage current, spectroscopic ellipsometry, atomic force microscopy, Organic molecular beam deposition.

1. INTRODUCTION

Based on the versatility including response time, stress-strain behavior, and low energy consumption [1], dielectric elastomer transducers (DET) are promising candidates to mimic the natural muscle functionality including their rapid feedback mechanism within the human body [2]. DETs for biomimetic implants still face the challenge to realize a significant reduction of the actuation voltages [3, 4]. One approach to follow is reducing the elastomer film thickness. Silicone-based polymer films, prepared by spin-coating, are limited to micrometer thickness and require operation voltages of several hundreds of volts to reach strains of 25 % to 48 % [5]. Alternate-current electro-spraying (ESD) of

polydimethylsiloxane (PDMS) in solution has been presented as cost-effective and fast alternative to realize sub-micrometer-thin elastomer membranes [6, 7]. Deposition rates by one order of magnitude increased compared to molecular beam deposition (MBD) have been acquired [8]. However, these growth rates result in micrometer-rough surface morphologies formed by isolated PDMS-droplets for membrane thicknesses below 600 nm [6, 7]. Thus, fabricated by ESD nanometer-thin DETs for low-voltage operation have not been realized so far.

In contrast, based on MBD this approach of low-voltage nanometer-thin DETs has been developed to high maturity. A proof-of-principle, reaching strains up to 6 % at medically-approved voltages for implants, has been delivered on the basis of a 200 nm-thin PDMS membrane [9]. Furthermore, by means of MBD the functional group density and chain length of polydimethylsiloxane (PDMS) is tailored and thus, intended to enable for the manipulation of the elastomer's elasticity and chemical integrity [8]. To enhance the dielectric strength of the elastomer intentionally synthesized PDMS functional groups have been realized and applied to MBD [10]. Regarding the nanometer-thin DETs long-term reliability, adhesion layers on the basis of tailored thiol-PDMS between electrode and elastomer layer have been introduced and optimized by means of spectroscopic ellipsometry (SE) [11]. Hereby, SE is a versatile tool, which enables to follow the plasmonic fingerprints during the growth of the multilayer elastomer/metal nanostructures. Furthermore, SE online monitoring allows for the control of morphology and film thickness with nanometer precision – an unremitting requirement for DET nanostructures. The demonstration of low-voltage DETs by MBD has drawn a great interest within the community [12]. So far, the elastomer membranes utilized for DETs have film thicknesses above 3 µm [13, 14], which points out the pioneer role of MBD processing regarding polymer thin-film technology.

The excellent elasticity of cross-linked PDMS combined with its biocompatibility, makes it especially suitable for medical applications such as DET-based medical implants [15]. Hereby, linear siloxane-based PDMS offers the broadest range of molecular weights to be MBD tailored [8]. Cross-linking of PDMS can then be achieved through the presence of functional groups by applying ultraviolet (UV) radiation to force the photo-initiated reaction of radicals [16, 17]. The UV cross-linking of vinyl-terminated PDMS has been successfully shown [6, 9]. However, applying UV light curing after the fabrication of the polymer membrane leads to partially polymerized elastomer layers with a pronounced cross-linking gradient [18]. Therefore the *in situ* polymerization of the single polymer chains arriving on the substrate has been assembled [11].

For bulk materials, the elastic properties are usually determined by e.g. unconfined compression tests [19]. In case of soft nanometer-thin polymer films, asymmetric cantilevers have been utilized to describe their elastic/viscoelastic behavior under applied strain [20]. Exhibiting no predefinition of the structure to be characterized, AFM nano-indentation (NI) recently gained attention for the determination of mechanical material properties nano-scale polymer/metal structures [18, 21, 22]. Herein, we present the homogenous cross-linking of PDMS membranes with tailored elastic moduli down to a few hundreds of kPa – compliance comparable to that of natural muscle.

Embedded between compliant electrodes dielectric performance of elastomer membranes is validated based on leakage currents, which typically increase with electrostatic pressure. Their understanding is crucial to maintain the actuation efficiency for nanometer-thin DEAs compared to micrometer-thick DETs. Combined with homogeneity of better than 2 %, MBD under ultra-high vacuum conditions offers a reliable growth process for polymer membranes with lowest defect density possible. Still, membrane imperfections are unavoidable; for example micro-voids or impurities incorporated during the transfer into the vacuum atmosphere act as weak points in the dielectric. These localized spatial variations in the membrane's electronic properties eventually lead to local breakdowns. Thus, it is unlikely that DETs will reach its ideal breakdown strength given by the elastomer material's intrinsic properties. Electro-mechanical breakdowns can be shifted towards increased electric fields, if the DET membrane is pre-stretched [23], or charge control is used [24]. Within this study we report on the electric breakdown strength of substrate-based nanometer-thin DETs with varying membrane thickness. *Self-clearing* events, well known for micrometer-thick DETs [25, 26], are observed to clear-up local impurities by

thermally induced evaporation subsequently reanimating the low-voltage DET functionality.

Due to the fact, that a nanometer-thin DET with an active area of square-centimeters create forces of only about 10^{-4} N [9] multilayered DETs with a few thousand layers would be required to mimic natural muscle forces. Therefore, the crucial stiffening effect of multilayered DETs will be discussed on the basis of a single- and dual-layered nanometer-thin DETs deposited on single-crystal silicon. Typically, the determination of DET actuation characteristics is relying on either expansion measurements of free-hanging membranes or on asymmetric substrate-based structure characterized by cantilever bending [9, 20, 27]. Here, we present AFM measurements in contact mode to vertically follow the DET actuation.

2. EXPERIMENTAL

2.1 Nanometer-thin dielectric elastomer membranes prepared by thermal evaporation

Supplied materials were thermally evaporated and deposited under ultra-high vacuum (UHV) conditions at a base pressure of 10^{-7} mbar, see Figure 1. DMS-V05 (Gelest Inc., Morrisville, PA, USA) and synthesized SH-PDMS [11] were evaporated using low-temperature effusion cells (NTEZ, Dr. Eberl MBE Komponenten GmbH, Weil der Stadt, Germany) with a 25 cm^3 crucible for DMS-V05 and a 2 cm^3 crucible for SH-PDMS. DMS-V05 thin films were evaporated at a crucible temperature between (190 ± 5) and (205 ± 5) °C, SH-PDMS at a temperature of 130 °C, well below the thermal degradation temperature of vinyl and thiol end groups, respectively [8, 28]. High-temperature effusion cells (HTEZ, Dr. Eberl MBE Komponenten GmbH, Weil der Stadt, Germany) with 10 cm^3 PBN-crucibles were utilized to evaporate 20 nm-thin Au electrodes at a temperature of 1440 °C, corresponding to a deposition rate of about 1.1 10^{-2} nm s^{-1}. The Si-substrate with 100 nm SiO_2 coating (Siegert Wafers GmbH, Germany) was mounted at a distance of 400 mm away from the crucibles and the UV lamp.

UV cross-linking was initiated by *in situ* irradiation from an externally mounted source (H2D2 light source L11798, Hamamatsu, Japan) through a CaF_2-window [29]. The spectrum of the deuterium UV lamp ranges from 160 to 400 nm, with a peak intensity at a wavelength of approximately 190 nm. The preferential pathway via the radicalization of vinyl-groups is accompanied by side group radicalization, see Figure 1(e) [9]. At irradiation wavelengths below 190 nm methyl groups become sensitive to radicalization. C-H or even Si-C bonds are radicalized and methyl side groups are separated from the Si-O backbone of the PDMS chain [9, 30, 31].

The absolute thickness of the UV-cured PDMS film was determined using the spectroscopic ellipsometer SE801 (Sentech Instruments GmbH, Berlin, Germany) and crosschecked via atomic microscopy surface scans along intentionally induced scratches. To *in situ* examine the optical properties of the forming nanostructures *SpectraRay3* software was utilized. Spectroscopic Ψ- and Δ-values in the range 190 to 1050 nm were monitored at a frequency between 0.5 to 2 Hz at an incident angle of 70° to the normal of the substrate's surface. The 4 mm-wide incident beam resulted in a 4×10 mm^2 spot area on the substrate.

2.2 Optical and electrical characterization of nanometer-thin DETs

The electrical characterization setup for the leakage current determination consisted of two semi-spherical probe tips (SPA-3J, Everett Charles Technologies, Distrilec) mounted on micro positioners (Signatone, aps Solutions GmbH, Munich, Germany) to place the measurement tips on the DET's Au contact fingers individually. A contact between tip and specimen was realized by adding a liquid metal drop onto the tip (Coollaboratory Liquid Pro, Coollaboratory GmbH, Germany), see Figure 3(a). To apply the operation voltage and extract the leakage current trough the DET active area, a commercially available source meter (Keithley 2401) is employed. The *in situ* optical imaging of the Au-electrode surface for time-resolved observation of local breakdown and subsequent *self-clearing* events an optical light microscope (Stemi DV4 SPOT, Carl Zeiss AG, Feldbach, Switzerland) with an optical magnification of 50 was utilized. A Canon 700D camera is mounted with a minimal shutter time of 1/8000 s.

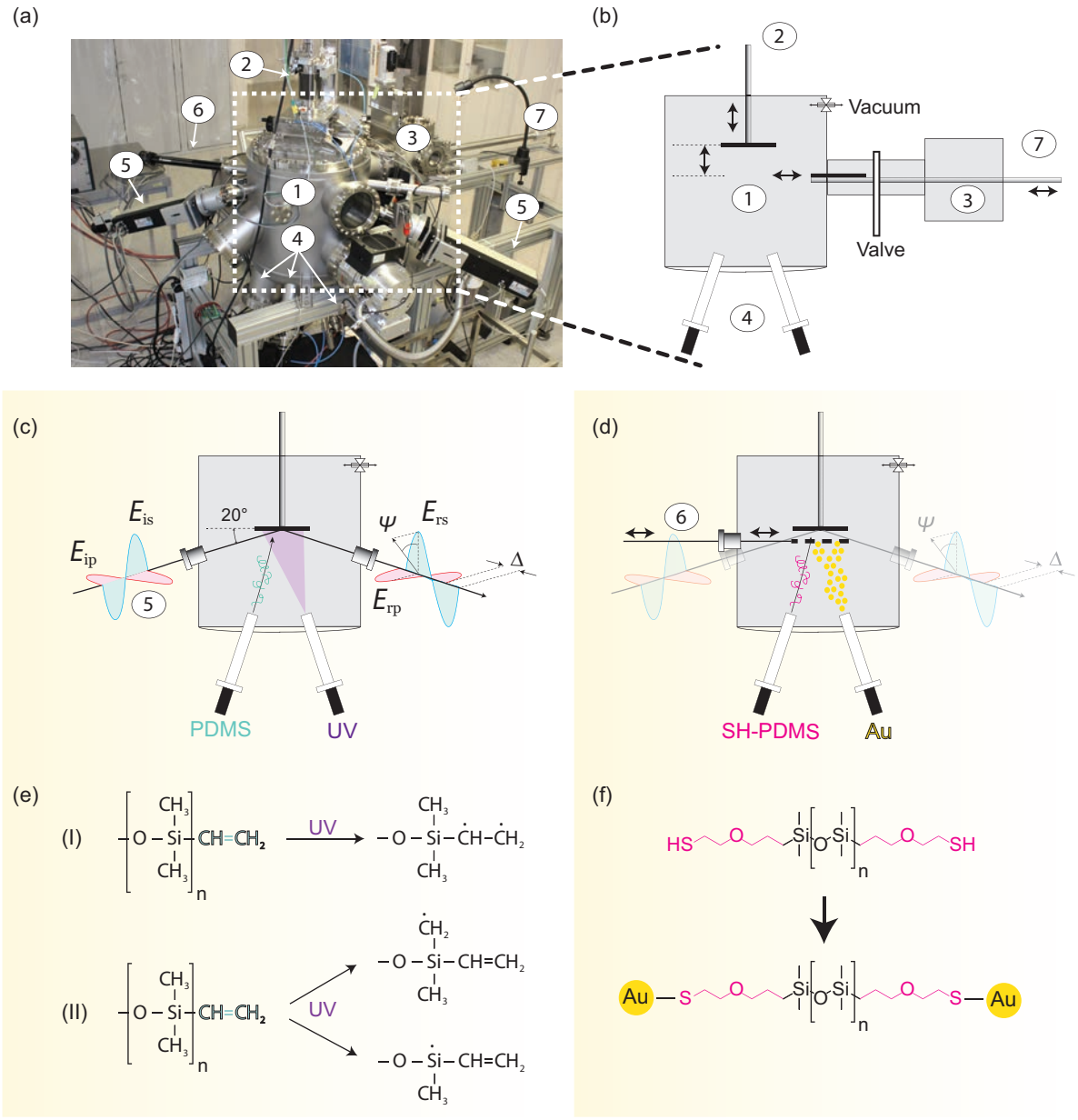

Figure 1. **(a,b)** Organic molecular beam deposition (OMBD) setup: Within the same ultra-high vacuum environment the substrate is introduced via the load-lock chamber (3) and transferred via a linear translator to the manipulator (2) within the process chamber (1). **(c)** The growth of polymer/metal from the evaporators (4) is online monitored with *in situ* spectroscopic ellipsometry (5). The nanometer-thin elastomer layers are *in situ* cured with UV light, while single PDMS chains are evaporated on the substrate. **(d)** The active area of the DET is defined via masking of the gold-electrodes inserted by the linear translators (6). Part **(e)** represents schematically the cross-linking mechanism between single chains of vinyl-terminated PDMS towards a 3D network of the elastomer membrane. Thiol-terminated PDMS (SH-PDMS) is utilized as adhesion interface for the gold electrode on PDMS. The covalent bonding of Au-thiol is schematically shown in part **(f)**. Multi-layered DET are realized through reliable repetition of these steps.

2.3 Atomic force microscopy for nano-indentation and actuation measurements on DET

For the nano-indentation experiments a FlexAFM ARTIDIS system (Nanosurf AG, Liestal, Switzerland) with B500_CONTR cantilevers (Nanotools GmbH, Munich, Germany) having a spherical carbon-tip of

(490 ± 15) µm diameter was utilized. Load-displacement curves of all samples were measured with a constant speed, while measuring the applied load. An indentation speed of 1 µm/s was set. The applied loads were adjusted between 50 to 200 nN to realize a constant indentation depth of about 100 nm. Thus, substrate effects can be neglected within the applied HERTZ model for elastomer membrane thickness of 500 nm. Nano-indentations were executed with 20 × 20 points corresponding on a spot size of 10 × 10 µm². The measured data were processed according to the HERTZ model, which is based on the classical Hertzian contact theory [19]. The elastic modulus of the soft polymer film can be expressed as given in Equation (1).

$$E_s = \sqrt{\frac{(1-\nu_s^2)^2}{6R}\left(\frac{dP}{dh}\right)^3 \frac{1}{P}} \tag{1}$$

The actuation of vertical actuation has been detected via the deflection of the same spherical carbon-tip of (490 ± 15) µm in scanning contact mode with applied force load of 8 nN. On a 10 × 10 nm² area scans were acquired with a speed of 20 ms per line with 256 lines in total.

3. RESULTS

3.1 Tailoring the elastic modulus of thermally evaporated, UV-cured, nanometer-thin PDMS membranes

Part (a) of Figure 2 presents characteristic sets of 400 nano-indentations on thermally evaporated and *in situ* UV-cured 500 nm-thin PDMS membranes. With increased growth rate from 98 to 253 nm/h a softened PDMS membrane with elastic modulus shifted from (10.5 ± 0.7) to (3.3 ± 0.3) MPa is observed. Within part (b) of Figure 2, a detailed analysis on the membranes elastic modulus with respect to the indentation depth (color map) is presented. Therefore, force loads of up to 500 nN have been applied to penetrate the PDMS network to a depth of up to 120 nm. Within the first 70 nm of indentation depth a potential decrease from (4.6 ± 0.6) to (4.4 ± 0.5) MPa is detected, whereas for increased penetration depth an asymptotic increase back to (4.6 ± 0.4) MPa is found. Thus, within the error bars resulting from the elastic moduli's distribution width, the *in situ* UV-cured PDMS membrane exhibits a constant elastic modulus within the first 120 nm of membrane thickness.

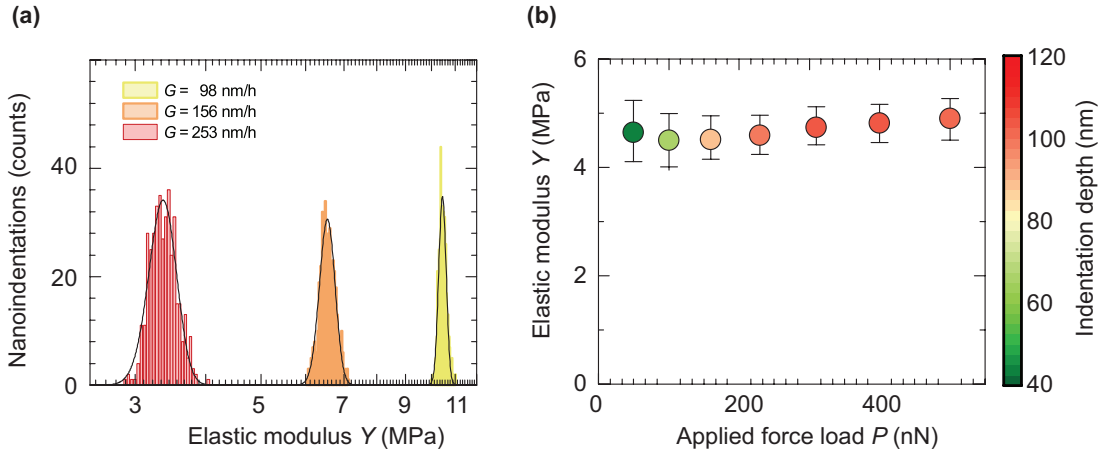

Figure 2. **(a)** Exemplary distributions of 400 nano-indentations each on 500 nm-thin PDMS membranes fabricated at growth rates ranging from 98 to 253 nm/h are presented. A Gaussian distribution is fitted to data to extract the full width half maximum. **(b)** The elastic modulus of a 500 nm-thin PDMS membrane is measured for applied force loads up to 500 nN. The color map describes the corresponding indentation depths of the AFM cantilever tip between 40 and 120 nm.

3.2 Breakdown and *self-clearing* of nanometer-thin DETs

Within Figure 3(a) the photograph characterizes an array of four active single-layer DET nanostructures with an active area of 4 × 16 mm² in size. The Au-electrodes are contacted via liquid metal droplets. The 100 nm SiO_2 layer on the 2-inch Si-wafer prevents a short cut between the two contacts of the upper and lower electrodes. A detailed leakage current study on a 200 nm-thin DET is shown in Figure 3(c) with respect to the applied voltage U and the corresponding electric field E. The grey-shaded area illustrates the resolution limit of the electronics down to the level of 0.1 nA. For applied voltages above 10 V (50 V/µm) an exponential increase of leakage current is detected, indicated by the red-colored fit function. The error bars characterize the influence of noise and long-term variations.

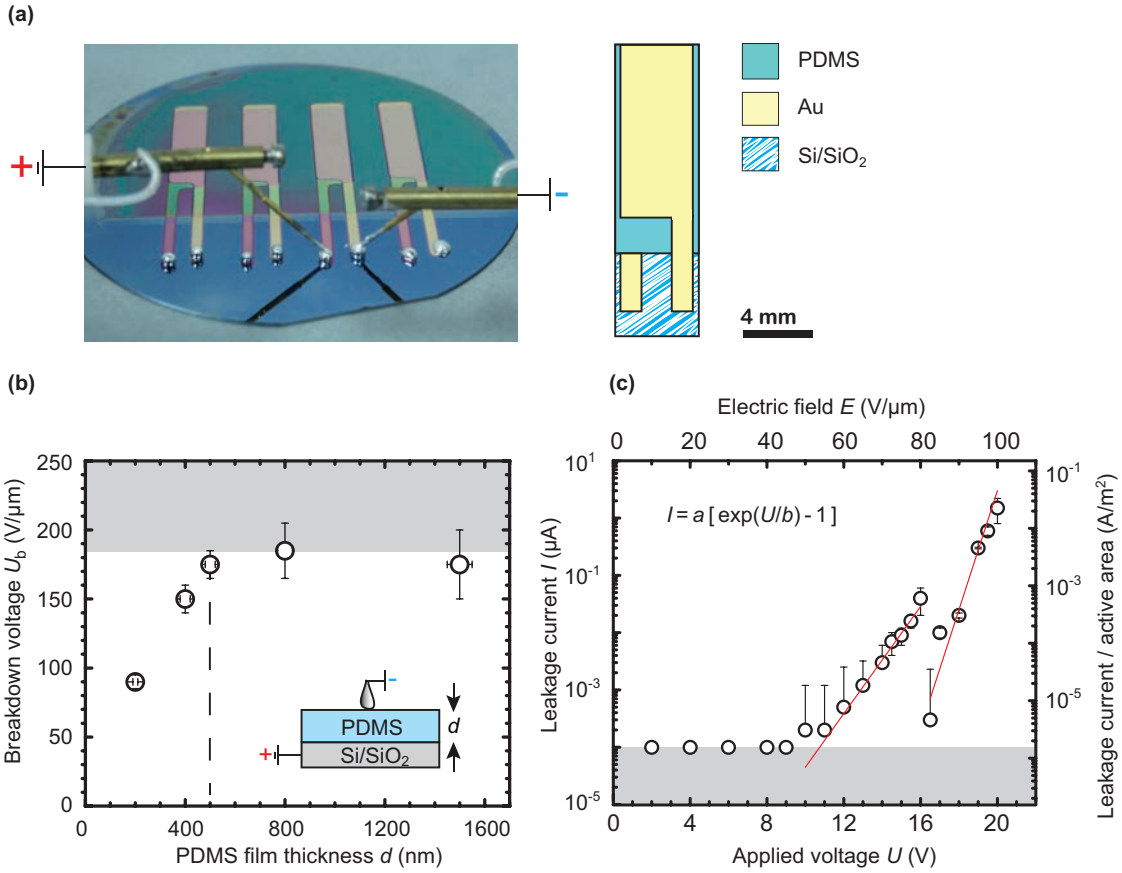

Figure 3. **(a)** Photograph of a four DET cantilever array on a 2-inch Si-wafer. The active DET areas defined by the Au electrode masks are 4 × 16 mm² in size. **(b)** The breakdown voltages are detected for PDMS membranes with thicknesses ranging from 200 to 1500 nm averaged over the 2-inch Si-wafer. The contact of the PDMS surface is realized with liquid metal droplets. The passivation SiO_2 layer on the wafer has been found to be 2.5 nm. The contribution of its breakdown voltage of 25 V/µm in this contact mode has been subtracted. **(c)** The leakage currents of a 200 nm-thin DET structure, as shown in part (a), are logarithmically plotted with respect to the applied voltage. The resolution limit of the electronics below 0.1 nA is gray shaded. The increase of the leakage current is described with an exponential fit function $I = (4.8 \pm 2.2)\ 10^{21}[\exp(U/(0.41 \pm 0.05))\text{-}1]$ for applied voltages below 16 V and $I = (9.1 \pm 1.5)\ 10^{10}[\exp(U/(0.93 \pm 0.09))\text{-}1]$ for voltages above 16 V after local *self-clearing* occurred.

At applied voltages of 16 V (80 V/µm) a distinct drop in leakage current is measured after which the leakage current repeatedly exhibits an exponential increase with operation voltages up to 20 V (100 V/µm), at which terminal breakdown of the elastomer membrane occurs. The event of terminal breakdown is further resolved in Figure 3(b) for PDMS membranes with thicknesses ranging from

200 to 1500 nm. To neglect influences related to the Au-electrode deposition such as Au-diffusion into the PDMS the membrane is directly contacted via the Si-wafer and liquid metal droplets on the surface. For this purpose Si-wafer with a SiO_2 of only 2.5 nm in thickness are selected. An increase in breakdown strength from (100 ± 5) to (185 ± 10) V/µm for increased film thicknesses up to 500 nm is measured. With further increased membrane thickness the electric breakdown strength remains constant within its error bars. The increasing error bar with increasing PDMS membrane thickness results from increased film thickness inhomogeneity over the 2-inch wafer together with an increase in surface roughness.

An inspection by optical microscopy of local breakdown events on a 400 nm-thin DET is presented in Figure 4. The overlap of the upper and lower electrodes has been intentionally designed as a 3 × 12 mm² active area. At electric fields of up to 125 V/µm the DET nanostructure remains stable – no local breakdowns can be observed by optical means. For increased electric fields of 150 V/µm local destructions of the PDMS/Au nanostructure are resolved by the magnified inset. Craters with diameters between 20 to 100 µm occur indicating fast vaporization. The functionality of the residual active area remains stable after *self-clearing* of the major defect points. By further increasing the electric field a total breakdown of the overall electrode is induced.

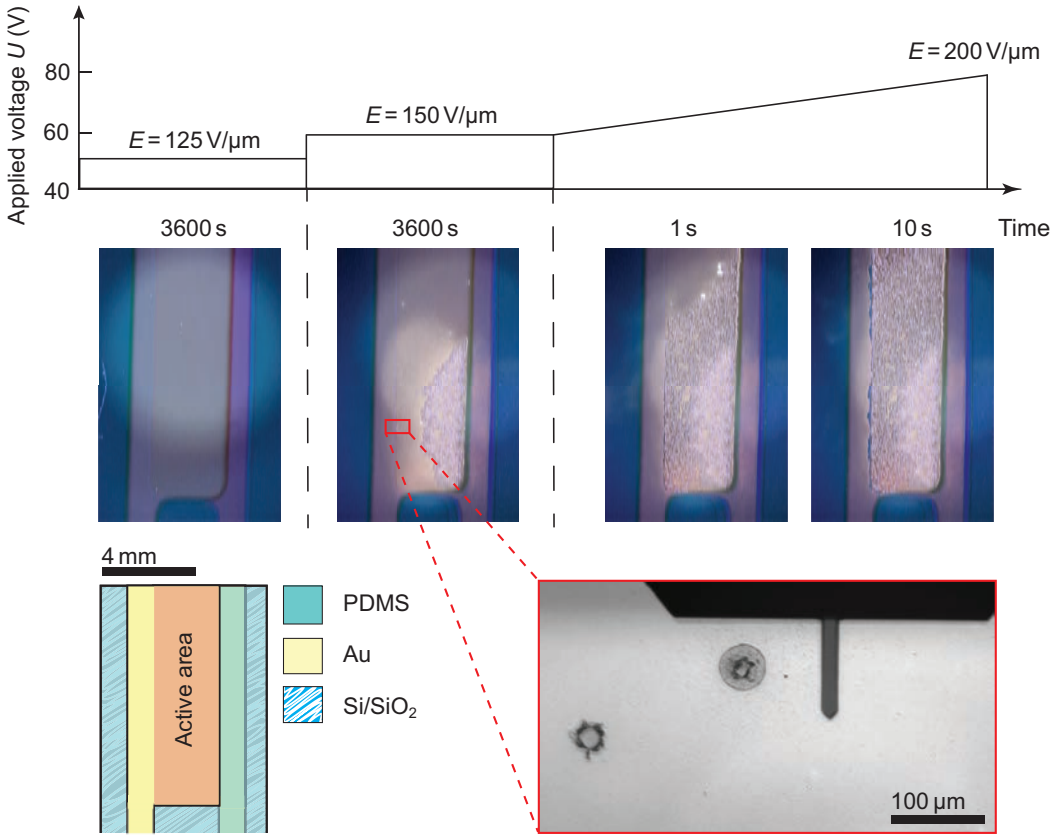

Figure 4. Optical microcopy resolves self-clearing for a 400 nm-thin single layer DET on a 3 × 16 mm² –sized active area defined by the overlap of lower and upper Au electrodes. At a breakdown voltage of 150 V/µm the evaporation of gold/PDMS at local defects leads to *self-cleared* breakthroughs. These local breakdowns asymptotically decrease with time resulting in about 30 % passive fraction of the former active DET area after an observation period of 1 hour. The magnification exhibits a mean diameter of (30 ± 5) µm for the self-cleared craters within the nano-membrane. With increased linear electric field up to 200 V/µm the *self-clearing* covers the whole active area of the DET cantilever already after a few seconds of applied voltage.

3.3 Strain and actuation efficiency of low-voltage nanometer-thin DETs

Atomic force microscopy surface scans served for the resolution of actuation perpendicular to the multilayered DET as shown in Figure 5. The force load of 8 nN enables to follow instantly the DET actuation with 20 ms resolution in contact mode. The reaction time of a 500 nm-thin and 1.2 MPa-soft DET is found to be within one line of the surface scan – thus it is stated to be below 20 ms. Relaxation to the maximum state of actuation is acquired within a few seconds.

These maximum actuation values are plotted with respect to the applied electric field E and to the ratio of electric field and elastic modulus E/Y in Figure 5(c). A clear dependency between detected strain and elastic modulus can be observed. Exemplarily, at an electric field strength of 100 V/μm the strain of nanometer-thin DET with elastic moduli of (11.2 ± 1.2), (6.5 ± 0.9), and (2.2 ± 0.5) MPa is extracted to be (2.9 ± 0.5) %, (3.9 ± 0.5) %, and (6.5 ± 0.5) %, respectively. A second-order polynomial describes the DET actuation. A distinct increase of the polynomial's linear fraction from (0.015 ± 0.001) to (0.044 ± 0.005) %/(V/μm) is observed the softer the PDMS membrane becomes. When scaled with the elastic modulus Y of the PDMS membrane the acquired strain at selected E/Y ratios is increasing for the DET with stiffened membrane. Again, a reduced breakdown strength for DET samples with PDMS membranes thinner than 500 nm is observed.

The maximally acquired strains for a single- (dots) and dual-layer (stars) DET, based on 500 nm-thin and 1.2 MPa-soft membranes are compared in Figure 5(d). A maximal vertical actuation of 35 nm corresponding to a strain of 8.5 % for a single-layer DET and 55 nm maximum vertical actuation corresponding to a strain of 5 % per active layer within the dual-layer DET is detected. The maximum strain for the dual-layer DET is measured at an electric field of 290 V/μm (145 V applied voltage), which is doubled compared to the maximally applied electric field of 150 V/μm (75 V applied voltage) for the single-layer DET.

4. DISCUSSION

The precise temperature control of MBD allows for stable evaporation rates of single PDMS chains to form nano-membranes with thicknesses of a few hundreds of nanometers. With increasing growth rate while constant UV-irradiation power is applied, the UV-irradiation density per PDMS chain arriving on the substrate is reduced, which leads to a reduced cross-linking in the membrane.

Manufactured as 200 nm-thin PDMS membrane between adherent SH-PDMS/Au-electrodes, such a DET exhibit leakage currents below 10^{-9} A for operation voltages below 8 V (40 V/μm). The distinct drop in leakage current at operation voltages of 16 V (80 V/μm) is related to a local breakdown event. A corresponding leakage current per active area of 10^{-3} A/m² is detected. This leakage current is comparable to that of micrometer-thick, 16 times pre-stretched VHB foil at same electric fields [32]. The terminal breakdown occurs at an electric field of 100 V/μm. Compared to a recently presented 200 nm-thin DET [29], for which its PDMS membrane has been UV-cured after the thermal evaporation in vacuum, we report increased breakdown voltages compared to 60 V/μm by more than 65 %. We relate this significant increase to the reduced defect density within the PDMS membrane and the related interfaces to the Au electrode due to the fabrication under vacuum. PDMS membranes with thicknesses above 400 nm can sustain electric fields up to (185 ± 10) V/μm, which describes a 250 % increase compared to a 20 μm-thick silicone-based DET [27], which has been spin-coated under atmospheric conditions and even a 32 % increase compared to the dielectric strength reported by the supplier (Dow Corning Sylgard) [33]. For membranes with thicknesses above 500 nm these breakdown strengths are found to be constant and are therefore correlated to the actual intrinsic materials property of our thermally evaporated *in situ* UV-cured PDMS film. As depicted in Figure 4, the breakdowns are observed as localized explosive evaporation of the Au/PDMS nanostructure. As the nanoparticle density under vacuum conditions is significantly reduced, we may correlate the weak points within the PDMS membrane to PDMS voids incorporated during the evaporation process. Within such voids the lowered permittivity enhances the local electric fields and further accelerates electric charges responsible for the

leakage current [34]. Such localized discharging is expected to pronounce the heating induced by leakage currents, which subsequently leads to vaporization. However, the *self-clearing* of these localized weak points reanimates the functionality of the residual active area operating with leakage currents orders of magnitudes reduced.

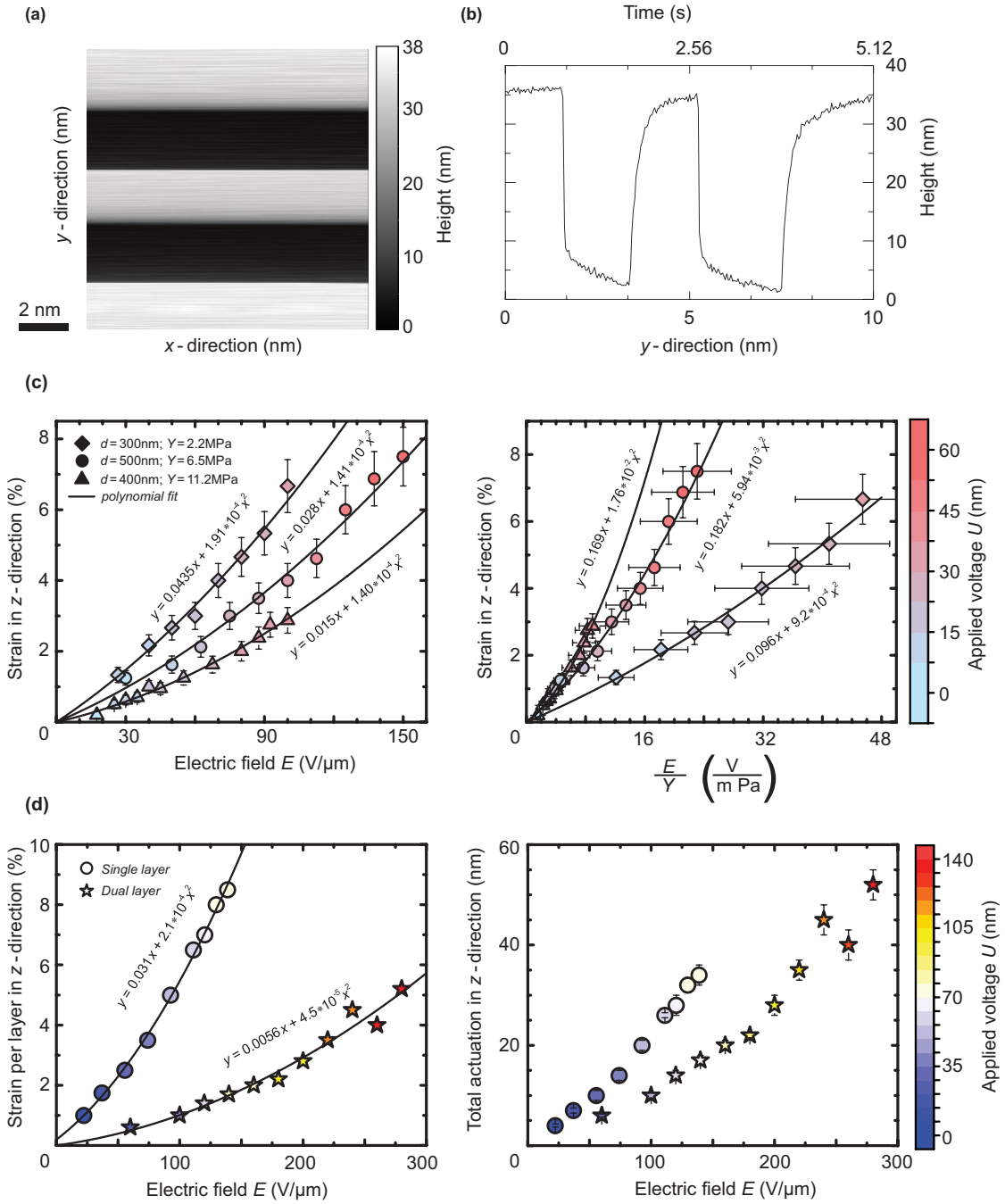

Figure 5. **(a)** Characteristic AFM 10 × 10 nm² (25.6 lines/nm) surface scan on a 500 nm-thin DEA operated at voltages of 75 V pulsed for about 1 Hz. The AFM tip with a radius of 490 nm moves in *y*-direction with a scanning frequency of 20 ms per line, which equals 0.512 s/nm. The *y*-directed cross-section is presented in **(b)**. The reaction time, associated with 90 % of maximal strain of the DEA, is determined to about 10 ms within one *y*-directed scanning line. Asymptotically it reaches maximum actuation of 35 nm after a few

seconds. **(c)** Vertical deformation in *z*-direction is plotted as the corresponding strain with respect to the applied electric field *E* and to the ratio of applied electric field and elastic modulus *E*/*Y* for substrate-based DET with selected PDMS film thicknesses and elastic moduli given by the legend inset. The strain with respect to the applied electric field can be described with polynomial function of second order. The color bar on the right side indicates the applied voltages of up to 75 V. **(d)** A comparison between a single-layer and dual-layer DET based on 500 nm-thin PDMS membranes with elastic modulus of 1.2 MPa is shown. The vertical strain per active layer and the corresponding vertical actuation is shown with respect to the applied electric field *E*. The color bar on the right side indicates the applied voltages of up to 140 V.

The nanometer-thin DETs presented exhibit reaction times below 20 ms subsequently requiring a few seconds to reach their maximum strain. Their final actuation strongly relates to the elastic modulus of the PDMS membrane. Although, with softened PDMS membrane the maximum acquired strain of the DET is enhanced, we calculated a reduced actuation with respect to the ratio of applied electric field and elastic modulus *E*/*Y*. Together with an increased linear contribution to the quadratic function, this behavior indicates an increasing stiffening influence of the metal electrodes the softer the PDMS membrane becomes. For the samples presented herein, their actuation should theoretically overlap with respect to the ratio *E*/*Y*. Contrary, an actuation shift by a factor of 1.4 and 2.8 for the DETs based on 2.2 MPa-soft and 6.5 MPa-soft PDMS membranes compared to the one based on a 11.2 MPa-soft PDMS membranes is induced by the electrodes stiffening.

This stiffening effect is underlined by the comparison of single- and dual-layer DET based on 500 nm-thin membranes. With an additional stacked active layer on top, the dual layer DET gains only 57 % in total actuation accompanied with a reduced strain per layer of 5 % compared to the vertical strain of from 8.5 % for a single layer DET. Moreover the dual layer DET requests for doubled electric field strength compared to the single layer DET to reach maximal strain. This may arise from interactions of inhomogeneous charge loads, which weaken each the stacked electric fields of the double layer. Clustering of gold particles with sizes of tens of nanometers instead of continuous layer-by-layer growth during thermal evaporation [11, 35] can explain localized charge variation on the nanometer-scale.

5. CONCLUSIONS AND OUTLOOK

As already proposed [8], based on MBD combined with *in situ* UV-curing the elastic modulus of PDMS nano-membranes can be tailored. We present hundreds of nanometer-thin PDMS membranes with elastic moduli down to 1.2 MPa. A further improvement towards pulsed *in situ* UV-irradiation will enable the manipulation of elastic moduli to a level of a few hundreds of kPa. This is an essential requirement to fabricate low-voltage DET nanostructures with compliances similar to them of human tissue.

To improve the breakdown strength of PDMS membranes for thicknesses below 500 nm we envision incorporating functionalized terminations for increased permittivity. This approach can enable the use of thicker membranes but still operate the related DET at voltages as low as 12 V. Furthermore, we expect that a pulsed UV irradiation will allow rearranging the arriving thermally evaporated PDMS chains on the membranes surface and fill up nano-voids. Avoiding such defects, we can reduce leakage currents and prevent local heating with subsequent breakdowns especially for a membrane thickness below 500 nm.

We proved the reaction times of low-voltage nanometer-thin DET to be in the millisecond range, comparable to micrometer-thick DET, which overlaps well with the vision to use them as medical implants as biomimetic artificial muscles or skin. A single 500 nm-thin, substrate-based DEA exhibits a maximum lateral strain of 4.2 %, which corresponds to strain-to-voltage-squared (s/V^2) ratio of 755 %/kV² - by far the highest reported (s/V^2)-value for thin-film DEAs. This performance metric has been found for 3 µm or even 30 µm-thick free-hanging membrane DEAs to be 125 %/kV² and 0.7 %/kV² [36], respectively, orders of magnitude reduced [13, 37, 38]. However, fabricated as multi-layers such nanometer-thin DET face significant stiffening, which reduces the actuation gain to only 57 % for a dual-layer DET and requiring double the electric field compared to single-layer DET. Additionally,

pronounced stiffening of the DET nanostructure occurs the softer the PDMS membranes becomes. This behavior requests for nanometer-thin stretchable electrodes combined with outstanding homogeneity.

ACKNOWLEDGMENTS

The authors are grateful to the financial support of the Swiss nano-tera.ch initiative *SmartSphincter* and of the Swiss Nanoscience Institute (SNI), University of Basel, Switzerland.

REFERENCES

[1] R. Pelrine, R. Kornbluh, Q. Pei *et al.*, "High-speed electrically actuated elastomers with strain greater than 100%," Science, 287(5454), 836-839 (2000).
[2] E. Fattorini, T. Brusa, C. Gingert *et al.*, "Artificial Muscle Devices: Innovations and Prospects for Fecal Incontinence Treatment," Annals of Biomedical Engineering, 1-15 (2016).
[3] Y. Bar-Cohen, [Application of Dielectric EAP Actuators] SPIE Press, Bellingham, 16 (2004).
[4] F. Carpi, D. Rossi, R. Kornbluh *et al.*, [Dielectric elastomers as high-performance electroactive polymers] Elsevier Ltd., Hungary, 2 (2008).
[5] A. E. Özçam, K. Efimenko, and J. Genzer, "Effect of ultraviolet/ozone treatment on the surface and bulk properties of poly(dimethyl siloxane) and poly(vinylmethyl siloxane) networks," Polymer, 55(14), 3107-3119 (2014).
[6] F. M. Weiss, T. Töpper, B. Osmani *et al.*, "Electrospraying Nanometer-Thin Elastomer Films for Low-Voltage Dielectric Actuators," Advanced Electronic Materials, 2(5), (2016).
[7] F. M. Weiss, T. Töpper, B. Osmani *et al.*, "Thin Film Formation and Morphology of Electrosprayed Polydimethylsiloxane," Langmuir, 32(13), 3276-3283 (2016).
[8] T. Töpper, S. Lörcher, F. Weiss *et al.*, "Tailoring the mass distribution and functional group density of dimethylsiloxane-based films by thermal evaporation," APL Materials, 4(5), 056101 (2016).
[9] T. Töpper, F. M. Weiss, B. Osmani *et al.*, "Siloxane-based thin films for biomimetic low-voltage dielectric actuators," Sensors and Actuators A: Physical, 233, 32-41 (2015).
[10] F. M. Weiss, F. B. Madsen, T. Töpper *et al.*, "Molecular beam deposition of high-permittivity polydimethylsiloxane for nanometer-thin elastomer films in dielectric actuators," Materials and Design, 105, 106-113 (2016).
[11] T. Töpper, S. Lörcher, H. Deyhle *et al.*, "Time-resolved plasmonics used to on-line monitor metal-elastomer deposition for low-voltage dielectric elastomer transducers," Adv. Elect. Mat., under revision, (2017).
[12] J. Bar-Cohen, WW-EAP Newsletter, 17(2), (2015).
[13] A. Poulin, S. Rosset, and H. R. Shea, "Fully printed 3 microns thick dielectric elastomer actuator," SPIE Smart Materials and Structure, 97980L, (2016).
[14] S. Rosset, and H. Shea, "Small, fast, and tough: Shrinking down integrated elastomer transducers," Applied Physics Reviews, 3, 031105 (2016).
[15] H. F. Mark, [Encyclopedia of Polymer Science and Technology] Wiley & Sons: New York, (2014).
[16] N. Tomer, F. Delor-Jestin, L. Frezet *et al.*, "Oxidation, chain scission and cross-linking studies of polysiloxanes upon ageings," Open Journal of Organic Polymer Materials, 2 (2), 13-22 (2012).
[17] U. Müller, H. J. Timpe, K. G. Häusler *et al.*, "Lichtinitiierte Polymer- und Polymerisationsreaktionen. 36. Mitt.: Photovernetzung vinlygruppenhaltiger Poly(dimethylsiloxane)," Acta Polymerica, 41 (1), 54-59 (1990).
[18] T. Töpper, F. Wohlfender, F. Weiss *et al.*, "Characterization of ultraviolet light cured polydimethylsiloxane films for low-voltage, dielectric elastomer actuators," Proc. SPIE 9798, 979821-10 (2016).

[19] F. Carrillo, S. Gupta, M. Balooch *et al.*, "Nanoindentation of polydimethylsiloxane elastomers: Effect of crosslinking, work of adhesion, and fluid environment on elastic modulus," Journal of Materials Research, 20(10), 2820-2830 (2005).
[20] T. Töpper, B. Osmani, F. M. Weiss *et al.*, "Viscoelastic properties of polydimethylsiloxane studied by cantilever bending," European Cells and Materials, 30, 68 (2015).
[21] B. Osmani, T. Töpper, H. Deyhle *et al.*, "Stress-induced soft metal-on-elastomer films," Science Advances, submitted, (2017).
[22] B. Osmani, H. Deyhle, F. M. Weiss *et al.*, "Morphology and conductivity of Au electrodes on polydimethylsiloxane using (3-mercaptopropyl)trimethoxysilane (MPTMS) as an adhesion promoter," Proc. SPIE, 9798, 979822-11 (2016).
[23] Bauer S. , and P. M., "Electromechanical characterization and measurement protocol for dielectric elastomer actuators," Smart Structures and Materials, 6168, (2006).
[24] T. A. Gisby, S. Xie, E. P. Calius *et al.*, "Integrated sensing and actuation of muscle-like actuators," Smart Structures and Materials, 7287, 728707 (2009).
[25] S. Ahmed, and Z. Ounaies, "A study of metalized electrode self-clearing in electroactive polymer (EAP) based actuators," SPIE, 9798, 97983F-9 (2016).
[26] B. Curdin, G. Samuele, A. Hatem *et al.*, "Inkjet printed multiwall carbon nanotube electrodes for dielectric elastomer actuators," Smart Materials and Structures, 25(5), 055009 (2016).
[27] B. Osmani, E. A. Aeby, and B. Müller, "Stress measurements of planar dielectric elastomer actuators," Review of Scientific Instruments, 87(5), 053901 (2016).
[28] A. Chandekar, S. K. Sengupta, and J. E. Whitten, "Thermal stability of thiol and silane monolayers: A comparative study," Applied Surface Science, 256(9), 2742-2749 (2010).
[29] T. Töpper, F. Weiss, B. Osmani *et al.*, "Siloxane-based thin films for biomimetic low-voltage dielectric actuators," Sensors and Actuators A: Physical, 233(0), 32-41 (2015).
[30] C. Dölle, M. Papmeyer, M. Ott *et al.*, "Gradual Photochemical-Induced Conversion of Liquid Polydimethylsiloxane Layers to Carbon Containing Silica Coatings by VUV Irradiation at 172 nm," Langmuir, 25(12), 7129-7134 (2009).
[31] L. Prager, L. Wennrich, R. Heller *et al.*, "Vacuum-UV irradiation-based formation of methyl-Si-O-Si networks from Poly(1,1-dimethylsilazane-co-1-methylsilazane)," Chemistry – A European Journal, 15(3), 675-683 (2009).
[32] T. A. Gisby, S. Q. Xie, E. P. Calius *et al.*, "Leakage current as a predictor of failure in dielectric elastomer actuators," SPIE, 7642, 764213-11 (2010).
[33] P. Brochu, and Q. Pei, "Advances in dielectric elastomers for actuators and artificial muscles," Macromol. Rapid Commun., 31(1), 10-36 (2010).
[34] L. A. Dissado, and J. C. Fothergill, "Overview of electrical degradation and breakdown," Electrical Degradation and Breakdown in Polymers, Lightning Source UK, Milton Keynes, 49-68 (2008).
[35] M. Hövel, B. Gompf, and M. Dressel, "Dielectric properties of ultrathin metal films around the percolation threshold," Physical Review B, 81(3), 035402 (2010).
[36] S. Rosset, and H. Shea, "Flexible and stretchable electrodes for dielectric elastomer actuators," Appl. Phys. A, 110(2), 281-307 (2013).
[37] S. Akbari, S. Rosset, and H. Shea, "Improved electromechanical behavior in castable dielectric elastomer actuators," Appl. Phys. Lett., 102(071906), (2013).
[38] S. J. Dünki, Y. S. Ko, F. A. Nüesch *et al.*, "Self-repairable, high permittivity dielectric elastomers with large actuation strains at low electric fields," Adv. Funct. Mater., 25, 2467-2475 (2015).

*tino.toepper@unibas.ch; phone 0041 61 207 54 45; fax 41 61 265 9699; www.bmc.unibas.ch